buildings

MDPI

Article

Effect of Blowing-Agent Depletion on Thermal Conductivity During Accelerated Thermal Aging of Polyisocyanurate Foams

Tomas Makaveckas [1,*], Andrius Jaskūnas [2], Raimondas Bliūdžius [3], Jurga Kumžienė [3] and Vilma Šipailaitė-Ramoškienė [4]

[1] Alytus Faculty, Kauno Kolegija, Seirijų g. 2, 62116 Alytus, Lithuania
[2] Faculty of Chemical Technology, Kaunas University of Technology, Radvilėnų pl. 19, 50254 Kaunas, Lithuania
[3] Institute of Architecture and Construction, Kaunas University of Technology, Tunelio g. 60, 44405 Kaunas, Lithuania
[4] Faculty of Informatics, Engineering and Technologies, Kauno Kolegija, Pramonės pr. 22, 50387 Kaunas, Lithuania
* Correspondence: tomas.makaveckas@kaunokolegija.lt

Abstract

Polyisocyanurate (PIR) insulation boards are widely used in buildings because of their low thermal conductivity, however their long-term performance is affected by aging. This study investigates the effect of accelerated thermal aging at +70 °C on the thermal conductivity and gas composition of pentane-blown PIR boards. Thermal conductivity was monitored over time, while changes in blowing-agent composition were analyzed using gas chromatography/mass spectrometry (GC/MS). Thermal conductivity increased from 0.0201–0.0211 W/(m·K) to 0.0243–0.0247 W/(m·K), corresponding to an increase of approximately 18–22%, with the most pronounced changes occurring during the first 40–50 days before stabilizing. GC/MS identified isopentane, cyclopentane, and pentane as the main gases in the foam cells, with isopentane as the dominant component. Accelerated aging caused a progressive decrease in blowing-agent concentration, explaining the deterioration in thermal insulation performance. Thermal outgassing proved more reliable than solvent extraction, providing higher sensitivity and reproducibility. Sample location, sample size, and outgassing temperature significantly affected the measured gas quantities, while higher outgassing temperatures improved analytical sensitivity without changing gas composition trends. The results confirm that the aging-induced increase in thermal conductivity is primarily caused by the loss of low-conductivity blowing agents, improving understanding of the long-term performance of PIR insulation materials.

Keywords: polyisocyanurate; thermal conductivity; accelerated thermal aging; blowing gas; thermal outgassing

Academic Editor: Apple L.S. Chan

Received: 9 July 2026
Revised: 2 August 2026
Accepted: 5 August 2026
Published: 6 August 2026

1. Introduction

With growing awareness of environmental sustainability, the construction industry has increasingly focused on materials that offer both high performance and low environmental impact [1]. Polyisocyanurate (PIR) foam, with its high thermal resistance, contributes to energy efficiency by reducing heating and cooling loads in buildings. However, the environmental sustainability of PIR foam is closely tied to the choice of blowing agents used in its production [2,3]. The thermal insulation capability of PIR foam largely stems from its cellular structure and the properties of the gases trapped within these cells. Typically, PIR foams consist of a high proportion of closed cells (92–98%) [4,5], which are filled

with blowing agents like pentane or hydrofluoroolefins (HFOs) that have low thermal conductivities compared to air. These agents replace air within the cells, significantly lowering the foam's thermal conductivity [6,7].

Blowing agents play a critical role in the production and performance of PIR foam. Pentane, a hydrocarbon, is commonly used due to its high molecular weight and low thermal conductivity, making it an effective insulator [8]. However, pentane is known to diffuse out of the foam cells over time, leading to a gradual degradation in the foam's insulation properties [9]. This aging is caused by the gradual diffusion of the low conductivity blowing agents out of the foam and the simultaneous infiltration of air, which has higher thermal conductivity [10]. Over time, as the blowing agent concentration inside the cells decreases and air concentration increases, the foam's overall thermal resistance drops [11]. This aging process is well recognized in construction standards and is often accounted for in building insulation performance evaluations [6,12]. Although standardized accelerated aging methods make it possible to estimate the expected changes in the thermal properties of PIR over time, these estimates are based primarily on modeling and accelerated aging tests. Consequently, their accuracy under actual operating conditions remains a matter of debate.

The slow diffusion of the blowing agents is a double-edged sword. While it ensures that the foam retains its insulating properties for an extended period, it also means that once the process begins, it is irreversible. Blowing agents like pentane provide excellent thermal resistance initially, but as air and moisture gradually replace the gas within the foam's cells, the thermal performance deteriorates. Thus, one of the most significant factors contributing to the aging of PIR foam is the escape of blowing agents and the ingress of air [6,13,14]. Various forms of pentane, such as isopentane and cyclopentane, are employed as physical blowing agents in PIR foam production, and their effectiveness in maintaining thermal resistance is a function of their molecular properties, particularly their low thermal conductivity and slow diffusion rates [6,13,15].

Aging in PIR foam is a multifaceted process that can be attributed to several factors, the most prominent being the diffusion of the blowing agents and the intrusion of air [6]. This process begins immediately after manufacturing and progresses over time, albeit at varying rates depending on the gas composition, foam density, and external conditions such as temperature and humidity [6,14]. The aging process can also be accelerated by environmental factors such as temperature fluctuations and moisture. Exposure to high temperatures increases the diffusion rates of blowing agents, thereby speeding up the aging process. Moisture ingress further exacerbates the degradation of thermal performance by increasing the foam's thermal conductivity, as water has a higher thermal conductivity than both air and the typical blowing agents used in PIR foams [6,12,15,16].

To mitigate the effects of aging and ensure accurate predictions of insulation performance over time, several accelerated aging methods have been developed. These methods simulate long-term aging by subjecting the foam to elevated temperatures or by slicing the foam to reduce diffusion paths, thereby increasing the rate at which gases escape and air infiltrates. This allows researchers and manufacturers to assess the long-term thermal performance of PIR foam within a shorter timeframe [14]. Standardized testing methods also account for the aging process in determining the rated thermal properties of insulation materials. In the construction industry, it is crucial to ensure that the thermal resistance values reflect the long-term performance of insulation materials. The European and international standards that govern insulation testing have adopted accelerated aging methods, such as heat acceleration and slicing techniques, to assess the thermal conductivity of foams after a simulated aging period [14]. The use of these methods provides valuable data that allows architects and engineers to predict the thermal performance of buildings over their

entire service life. This is critical for the design of heating, ventilation, and air conditioning (HVAC) systems, as well as for ensuring the energy efficiency of buildings [5,13,14]. At the same time, there is a strong interest in the changes in the physical properties of these polymers through the determination of changes in pentane concentration in aging PIR foams [7]. These limitations highlight the need for the development of experimental methods for determining the concentration and composition of blowing gases in PIR foams during aging.

In the recent literature, the deterioration of the thermal properties of PIR is most often attributed to the diffusion of off-gases, their replacement by air, and the effects of moisture [17]. However, some authors note that these explanations are, in many cases, still based on theoretical assumptions, diffusion models, or accelerated aging tests [13]. Direct experimental evidence does exist, but its interpretation is limited by the discrepancy between laboratory conditions and actual service conditions, differences in measurement methods, and the complexity of determining gas migration within a closed-cell structure.

The thermal conductivity of PIR foam is influenced not only by the type and concentration of gases in the cells but also by other structural factors such as cell size, distribution, and anisotropy [13,18,19]. The cellular morphology, including porosity, cell size, and strut content, governs the heat transfer through the foam by influencing both the gas conduction and radiative heat transfer mechanisms [6,20]. More closed cells are desirable as it minimizes convective heat transfer, allowing PIR foam to achieve thermal conductivities as low as 0.020 W/m·K, which is superior to many other conventional insulation materials like mineral wool or polystyrene [6,20]. The size of the foam cells plays a significant role in determining the material's effective thermal conductivity [21]. Smaller cells typically reduce heat transfer by radiation and limit convective heat flow, leading to better insulation performance. Foams with predominantly closed cells are less susceptible to convective currents, thus maintaining lower thermal conductivity compared to open-cell foams of the same size [12].

Despite considerable research on the thermal aging of PIR foams, important knowledge gaps remain regarding the direct experimental determination of blowing-agent composition during aging and its relationship with thermal conductivity. Previous studies have primarily focused on thermal conductivity measurements, diffusion modeling, and accelerated aging procedures, whereas comparatively few have combined thermal characterization with quantitative GC/MS analysis of blowing gases. Furthermore, the analytical methodologies used for determining blowing-agent composition in aged PIR foams have received only limited comparative evaluation. Therefore, the aim of this study was to investigate the influence of accelerated thermal aging at 70 °C on both the thermal conductivity and the blowing gas composition of pentane-blown PIR insulation boards. Thermal conductivity measurements were combined with GC/MS analysis to quantify blowing-agent depletion during aging, while thermal outgassing and heptane extraction were systematically compared to evaluate their suitability for qualitative and quantitative gas analysis. This combined experimental approach provides direct evidence linking blowing-agent depletion with deterioration of thermal insulation performance and offers practical recommendations for reliable gas analysis of aged PIR foams.

2. Materials and Methods

This section describes the methodology for accelerated thermal aging and gas composition analysis of PIR thermal insulation boards. The aim of the study was to evaluate how long-term exposure to elevated temperatures affects the material's thermal conductivity coefficient and the composition of the foam gas present in the pores. To this end, thermal conductivity measurements were performed on samples aged for varying durations at

a temperature of +70 °C using a FOX 314 heat flux meter. Accelerated thermal aging at 70 °C was selected because elevated temperature conditioning is a well-established method for simulating long-term diffusion of blowing agents in closed-cell polymer foams and is widely adopted in previous studies and European standards for evaluating the long-term thermal performance of PIR insulation materials [14,22]. To determine the possible causes of changes in thermal properties, the composition of the gas phase in the pores was additionally investigated using liquid extraction and thermal outgassing methods. Gas chromatography and mass spectrometry (GC/MS) analysis was used to identify and quantitatively assess the gas components. The results of these studies allow for an assessment of the impact of thermal aging on the performance properties of PIR panels and a better understanding of the mechanisms underlying changes in thermal conductivity as the material ages.

2.1. Products and Samples Used for Thermal Aging and Measurement of Thermal Conductivity

Before determining the gas concentration in the PIR pores, accelerated aging of the samples was carried out to investigate the effect of accelerated thermal aging on the thermal conductivity coefficient. For this experimental study, PIR (blown with pentane) rigid boards with aluminized multilayer facing were obtained from the producer. Seven identical 305 × 305 mm samples from the same 50 mm thickness PIR board were cut.

A heat flow meter FOX 314 (developed by TA Instruments, New Castle, DE, USA) was used to measure the thermal conductivity of the test products. The apparatus consists of two plates containing heat flow meters and temperature sensors located above and below the sample. The principle of the FOX heat flux meter measurements is to create a constant temperature difference between the lower and upper plates and to measure the specific heat flow and surface temperatures at a constant temperature. The FOX 314 heat flow meter has a plate size of 305 mm × 305 mm and a measuring area of 100 mm × 100 mm. The measuring plates and the sample of the FOX 314 instrument are insulated on all sides with a 30 mm thick coating with a calculated thermal resistance of approximately 0.96 (m^2·K)/W. The temperature control accuracy of this meter is ±0.01 °C and the absolute thermal conductivity accuracy is ±2%. This instrument was chosen because of its small sample size and has been used to investigate changes in the thermal conductivity of PIR samples after exposure to a temperature environment [23]. It was considered that lateral heat leakage is possible when measuring a small area and low thermal conductivity samples, but at this stage of the study, it is more important to determine the change in thermal conductivity after accelerated aging rather than the absolute thermal conductivity of the material under investigation, thus avoiding systemic lateral heat loss effects.

The samples for the investigation of changes in the thermal conductivity after exposure in +70 °C temperature environments were kept in such order: the thermal conductivity of all seven samples was measured after cutting them out, the first sample was set aside for gas analysis, the thermal conductivity of the second sample was measured after 30 days of conditioning at +70 °C, the third sample after 40 days, the fourth sample after 50 days, the fifth sample after 60 days, the sixth sample after 70 days, and the seventh sample after 80 days. Each accelerated thermal aging duration was represented by one PIR board specimen. The initial thermal conductivity of all specimens was measured prior to thermal aging in order to verify the uniformity of the material before assigning individual specimens to different thermal aging periods. The thermal conductivity coefficient of each sample is measured after each heat treatment cycle. All samples were conditioned at a controlled temperature and relative humidity climate chamber within 23 ± 3 °C and within 50 ± 10% relative humidity limits before measuring their thermal conductivity. The conditioning time of the samples before measurement under standard conditions was 24 h. When

determining the aged values of thermal conductivity, they are rounded to 0.0001 W/(m·K) as specified in the PIR product standard EN 13165 [22].

2.2. Preparation of Samples for Gas Analysis

The aim of this experiment is to investigate the blowing agent gas concentration in PIR pores after thermal aging at +70 °C for a certain time. Qualitative and quantitative analysis of a pentane mixture would provide a chemical explanation for the changes in the thermal insulation properties of PIR boards as they age. There is little information in the literature regarding the analysis of thermal insulation boards, as it is difficult to quantitatively collect gaseous components from the solid phase. Therefore, the aim of this study is to investigate changes in the composition of the gas phase during accelerated aging, while comparing the two most commonly used methods for analyzing PIR foam—liquid extraction and thermal outgassing. In both cases, gas-phase headspace analysis was performed on the samples, thus ensuring convenient sample collection. Liquid extraction was carried out using heptane as a solvent, which is nonpolar and perfectly compatible with the universal nonpolar capillary column used in gas chromatography. During the extraction, the solid sample was disintegrated in 5 mL of heptane to ensure pentane release, dissolution in the liquid phase, and mixing. Meanwhile, thermal outgassing was carried out in an oven for two hours at a temperature not exceeding 100 °C, as it represents the thermal stability limit for most polyurethane foams. At higher temperatures, thermal degradation products may form and contaminate the test sample. Since the tests were conducted multiple times, the average values of the results were calculated during data processing, and for the purpose of data comparison, all quantitative values are presented after being converted to 1 mg of solid PIR foam sample.

2.3. Gas Analysis

Pentane mixture components were separated and analyzed using gas chromatography and mass spectrometry. A PerkinElmer Clarus 500 gas chromatograph and PerkinElmer Clarus 500 mass spectrometer system (GC/MS) were used for this purpose. A universal capillary column, the COL-ELITE 5MS, was selected for chromatography. The column is 30 m long, has an inner diameter of 0.25 mm, and features a 0.25 mm thick layer of nonpolar adsorbent. Isothermal chromatographic conditions were selected for the separation of all tested samples with constant temperature—40 °C. Carrier gas—He (purity 99.999%)—was split in the injection port at 1:20 ratio and was supplied through the chromatographic column at a constant rate of 1 mL/min. Mass spectra were obtained by electron ionization, using a standard electron beam energy of 70 eV. Mass fragments with m/z values between 8 and 200 were recorded by the mass spectrometer. Substance concentrations were determined using the internal standard method. The NIST computer database was used for compound identification.

Quantification of components was performed by method of external calibration curves which were constructed using standards—pentane (Sigma Aldrich, anhydrous, ≥99%), 2-methylbutane (Sigma Aldrich, anhydrous, ≥99%), and cyclopentane (Sigma Aldrich, synthesis grade, ≥99%). All standards were analyzed using the same operating conditions using five concentrations levels—50, 100, 300, 500 and 1000 mg/m^3—to cover wider region of various concentrations. Linear regression of five concentration points yielded coefficients of determination (R^2) greater than 0.99 for all three compounds. Detection and quantification limits were calculated using signal to noise (S/N) ratio. Detection limits (S/N = 3) for pentane, isopentane, and cyclopentane were 1.43, 1.61, and 1.15 mg/m^3 respectively, while quantification limits (S/N = 10) for pentane, isopentane, and cyclopentane were 4.76, 5.37, and 3.82 mg/m^3 respectively. Repeatability was evaluated by three replications of

a standard mixture injections, which gave relative standard deviations lower than 3% for all measurements.

2.4. Optical Microscopy

The microstructure of selected PIR foam samples was examined using an optical microscope Zeiss SteREO Discovery.V12 (Oberkochen, Germany). The optical microscope is equipped with motorized 12× zoom which was utilized for high magnification and depth perception of foam cross-sectional cuts at a magnification of 110×. Cross-sections were prepared by cutting the specimens perpendicular to the board surface using a sharp blade in order to minimize damage to the cellular structure. Images were obtained for the unaged specimen (Sample 1) and for the specimen aged for 80 days at 70 °C (Sample 7). The observations were used for qualitative comparison of the cellular morphology, including cell size uniformity, cell wall integrity, and possible structural defects induced by thermal aging.

3. Results and Discussion

3.1. Thermal Conductivity Coefficient Dependence on Accelerated Thermal Aging

The results obtained by measuring the thermal conductivity coefficient before and after thermal aging the PIR samples are presented in Table 1. Each accelerated aging duration was represented by a single PIR specimen. The initial thermal conductivity coefficients of all seven PIR samples, measured immediately after cutting, showed a narrow range of values, varying from 0.02009 to 0.02112 W/(m·K) (Table 1). This limited variation indicates good manufacturing consistency of the tested PIR boards and confirms that the samples can be considered mutually comparable for the accelerated thermal aging study. The mean initial thermal conductivity value of the investigated samples was 0.02057 W/(m·K), with deviations not exceeding ±3%, which is typical for rigid PIR insulation products. These initial values were therefore taken as reference values for evaluating the effect of thermal aging at elevated temperature.

Table 1. Values of the thermal conductivity coefficients of PIR samples before and after thermal aging.

Sample No.	Initial λ Value, W/(m·K)	λ Value After Sample Accelerated Thermal Aging at +70 °C					
		After 30 Days	After 40 Days	After 50 Days	After 60 Days	After 70 Days	After 80 Days
1	0.02088						
2	0.02081	0.02257					
3	0.02072		0.02325				
4	0.02112			0.02460			
5	0.02011				0.02417		
6	0.02026					0.02466	
7	0.02009						0.02430

A pronounced increase in the thermal conductivity coefficient was observed after exposing the PIR samples to an elevated temperature of +70 °C, with the magnitude of change clearly dependent on the accelerated aging duration. After 30 days of conditioning at +70 °C, the thermal conductivity coefficient increased from an initial value of 0.02081 to 0.02257 W/(m·K), corresponding to an increase of approximately 8.5%. With further extension of the accelerated aging period to 40 and 50 days, the thermal conductivity continued to rise, reaching values of 0.02325 and 0.02460 W/(m·K), respectively. This stage is characterized by a relatively rapid increase in λ, indicating an intensive thermal aging process during the early exposure period.

For longer accelerated aging durations, from 60 to 80 days, the increase in thermal conductivity persisted but at a reduced rate. After 60 days of exposure, the measured thermal conductivity coefficient reached 0.02417 W/(m·K), while after 70 and 80 days, it stabilized in the range of 0.02430–0.02466 W/(m·K). Compared to the initial values, the total increase in thermal conductivity after prolonged thermal aging at +70 °C amounted to approximately 18–22%, depending on the individual sample. The reduced rate of change observed at extended thermal aging times suggests that the dominant aging mechanisms approach a quasi-stable state under the applied thermal conditions.

Overall, the results demonstrate that exposure of PIR insulation boards to elevated temperature leads to a systematic increase in thermal conductivity, strongly influenced by the duration of thermal aging. The most significant changes occurred during the first 40–50 days of exposure, followed by a gradual stabilization of λ values at longer accelerated aging times. Given that the primary objective of this study was to evaluate relative changes in thermal conductivity rather than absolute values and considering the declared measurement accuracy of ±2%, the observed trends are considered robust and representative of the thermal aging behavior of PIR materials under accelerated temperature conditions. The percentage change in the thermal conductivity coefficient (aged sample) relative to its initial value (fresh sample) is shown in Figure 1.

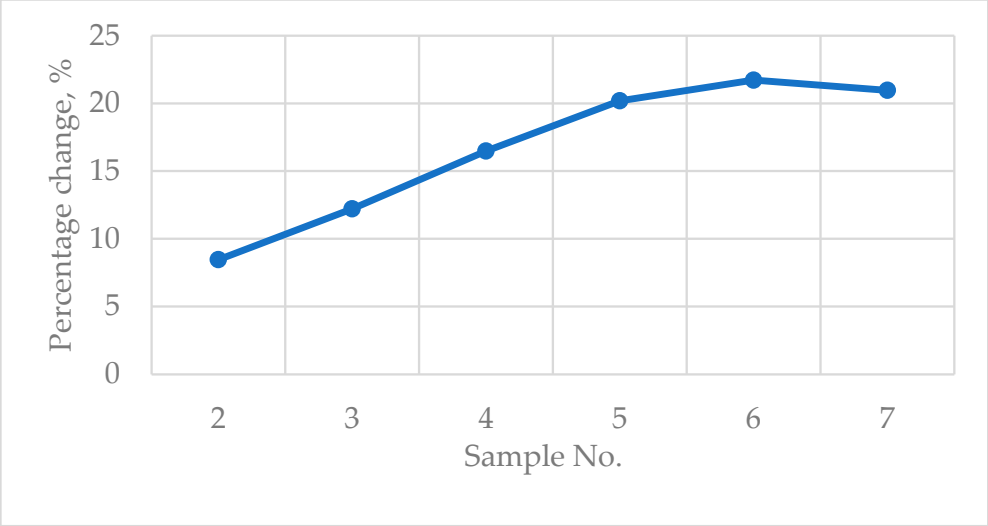

Figure 1. Percentage change in the thermal conductivity coefficient.

3.2. Identification and Analysis of Blowing Gas Composition

The composition of the gases used for PIR foaming and changes in their composition during the accelerated thermal aging of manufactured boards were determined using gas chromatography and mass spectrometry. The analysis identified three main gas components: isopentane, pentane, and cyclopentane. During the thermal outgassing tests, two additional impurities were detected—butane and dimethylbutane, which were neglected in this study.

Initially, the results of both sample preparation methods were compared using foam samples taken from different locations on the boards. Samples taken from the center and the edge of the boards were selected for comparison. The edges of the boards are less protected from environmental influences, so it is likely that the composition of their gas phase will change the most during accelerated aging. The results of the study, in which samples were heated for two hours in a sealed vial at 80 °C, with samples taken from the center of the board (17.5–19.9 mg per sample) and the edge (15.7–17.1 mg per sample), are presented in Figure 2.

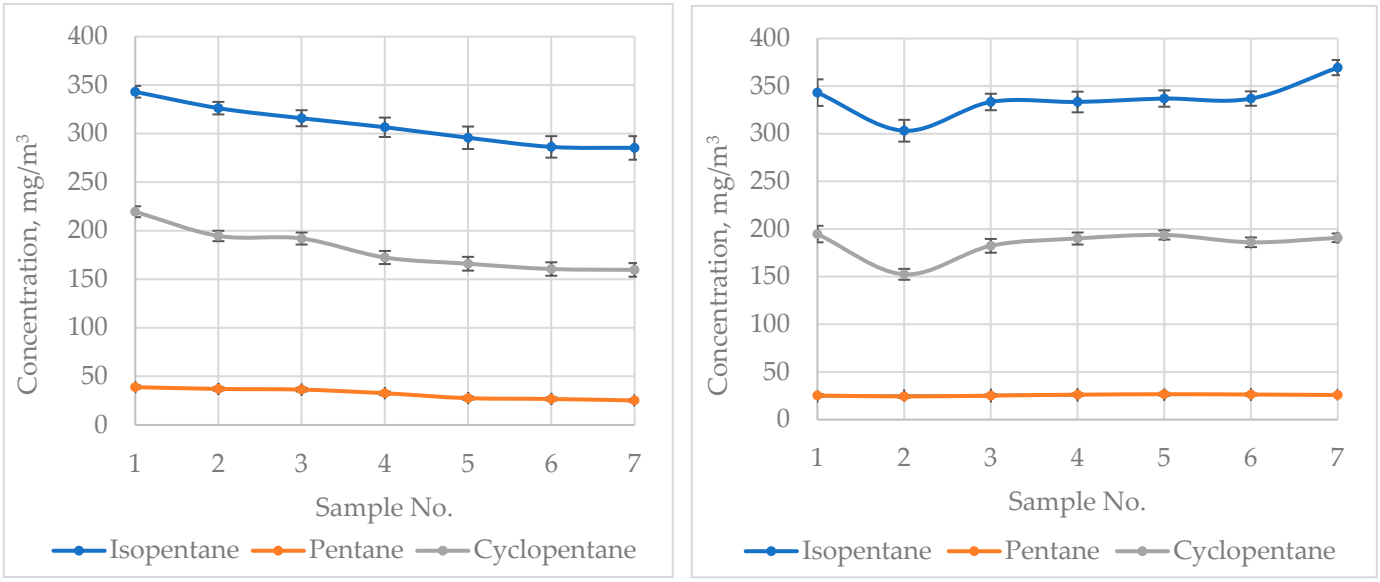

Figure 2. Changes in the gas-phase composition calculated per 1 mg of PIR foam after thermal outgassing of aged samples at 80 °C. (**a**) Sample taken from the center; (**b**) sample taken from the edge. Error bars indicate standard deviation.

Thermal outgassing results indicate that the headspace consists mainly of isopentane, while cyclopentane concentration is two times lower, which corresponds to the ratio of the gaseous components used in the foaming process (approximately 70% isopentane and 30% cyclopentane). The sample also contains pentane, but its concentration is more than 10 times lower than that of isopentane. It was also observed that samples aged for longer periods lose a portion of the pentane component in the blowing gas mixture. Samples taken from the center of the boards lose more isopentane, with its concentration decreasing from 343 to 285 mg/m^3, while the cyclopentane concentration decreases from 220 to 160 mg/m^3. Statistical calculations indicate that relative standard deviations for determined isopentane and cyclopentane concentrations do not exceed 8.8% and for pentane, they are up to 12.1%. It is interesting to observe that deviations slightly increase as boards age because of lower remaining concentrations of gases in the PIR samples. The results for samples taken from the edges of the boards vary too much, and the changes in gas composition are not consistent, although the concentrations are still comparable to those of samples taken from the center of the boards. The same trend was observed with relative standard deviations when they vary erratically up to 8.9% for isopentane and cyclopentane and up to 12.1% for pentane. This is because PIR at the edges of the boards is more exposed to the atmosphere and becomes more brittle. Consequently, the samples crumble more easily, making it harder to collect them in a manner suitable for analysis. Therefore, analysis is recommended only when samples are taken from the center of the boards.

Similar tests were conducted by disintegrating PIR samples in heptane and analyzing the resulting vapor phase above the solution. Samples were taken from the center (16.9–20.4 mg per sample) and the edge (15.1–16.8 mg per sample) of the boards. The test results are presented in Figure 3.

After heptane extraction, the concentrations of the components in the vapor phase are several times lower than after thermal outgassing. The ratio of the main components—isopentane and cyclopentane—has also changed; significantly less cyclopentane is detected when compared to pentane. This occurs due to the different solubility of both components in heptane. Isopentane is the most soluble because its branched structure results in the weakest intermolecular forces. Meanwhile, cyclopentane has strongest

intermolecular bonds and a highest boiling point, so its solubility in nonpolar heptane is lower. Pentane, on the other hand, falls in the middle between these two components in terms of solubility. Extraction samples taken from the center of the boards indicated a similar trend, which was observed in the samples after thermal outgassing—accelerated thermal aging decreased the amount of blowing agent. It resulted in a smaller release of pentane mixture into the headspace with the concentration of isopentane decreasing from 50 to 39 mg/m^3, and that of cyclopentane decreasing from 6 to 4 mg/m^3. It was expected that extraction would give higher statistical standard deviations because of the complexity of the method. Relative standard deviations were higher when compared to the thermal outgassing and were up to 11% for isopentane, up to 12% for pentane, and up to 13% for cyclopentane. Overall lower determined concentrations yielded higher dispersion of the results. In summary, it is evident that samples taken from the center of the boards yielded more consistent results than those taken from the outer edges. This was influenced by the thermal aging of foam, which becomes more porous and prone to decomposition.

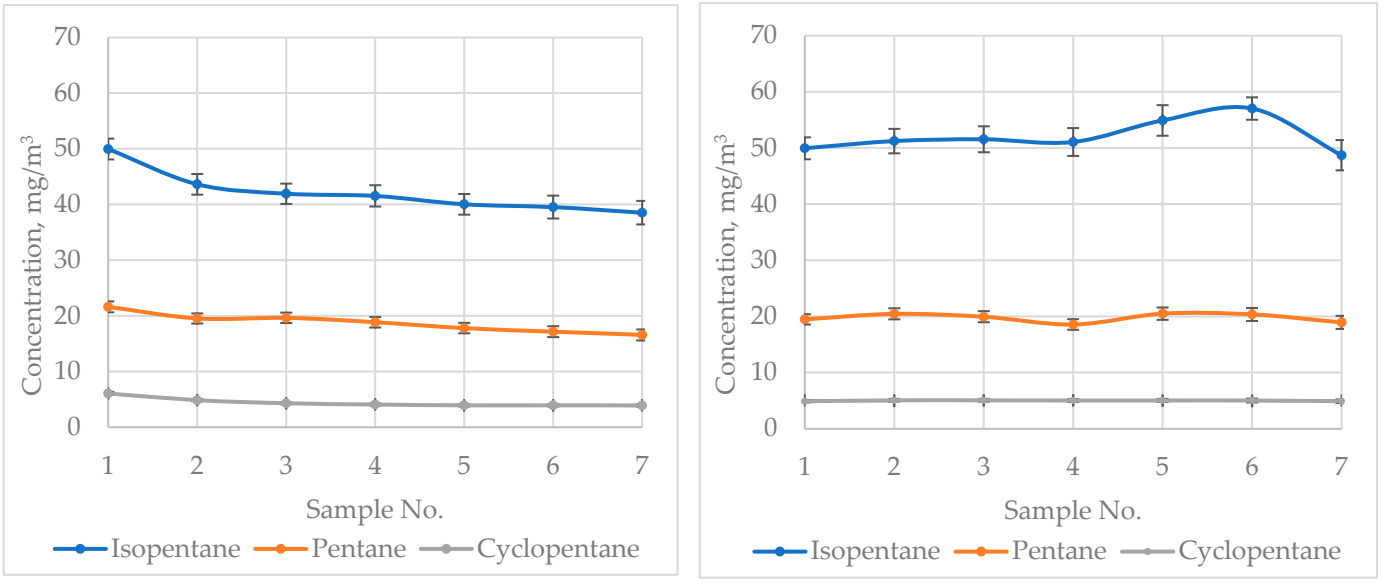

Figure 3. Changes in the gas-phase composition calculated per 1 mg of PIR foam after heptane extraction of aged samples with heptane. (**a**) Sample taken from the center; (**b**) sample taken from the edge. Error bars indicate standard deviation.

3.3. Analysis of Factors Affecting Blowing Gas Release

Both sample preparation methods are driven by interfacial phenomena occurring in heterogeneous systems and therefore should depend on the ratio between the gaseous, liquid, and solid phases. For this reason, additional experiments were conducted to determine the appropriate amount of solid material to be taken for analysis. All other analysis conditions remain the same. Thermal outgassing is performed at the same temperature of 80 °C using vials of the same size and analyzing PIR foam samples that vary in mass by approximately 2 to 2.5 times: 17.5–19.9 mg and 6.1–7.9 mg. The results, calculated as the mass of the released blowing agent per 1 mg of heated PIR foam, are presented in Table 2.

The results show that more gaseous components are released when a smaller mass of the heated sample is used, most likely due to the smaller surface area of the solid material relative to its volume. However, this applies only to the main components—isopentane and cyclopentane—since these components are relatively abundant in the solid phase. Detected pentane is present in the headspace only as an impurity, so the released amount depends very little on the mass of the heated sample. About 5% of the blowing agent is used in the

production of PIR foam, which corresponds to approximately 50 µg of gas per milligram of PIR material. As we can see, only a small portion of the gaseous components is released during thermal outgassing. A comparison of the headspace gas composition after thermal outgassing of PIR foam samples at 80 °C is presented in Figure 4.

Table 2. The mass of components released from aged PIR foam during thermal outgassing.

6.1–7.9 mg Samples				17.5–19.9 mg Samples			
Sample No.	**Isopentane, µg/mg PIR**	**Pentane, µg/mg PIR**	**Cyclopentane, µg/mg PIR**	**Sample No.**	**Isopentane, µg/mg PIR**	**Pentane, µg/mg PIR**	**Cyclopentane, µg/mg PIR**
1	4.517	0.285	3.242	1	3.329	0.378	2.130
2	4.061	0.276	2.606	2	3.165	0.360	1.889
3	3.948	0.265	2.446	3	3.064	0.353	1.863
4	3.887	0.256	2.464	4	2.975	0.317	1.673
5	3.798	0.245	2.352	5	2.870	0.268	1.610
6	3.715	0.238	2.291	6	2.778	0.260	1.558
7	3.547	0.223	2.103	7	2.768	0.245	1.549

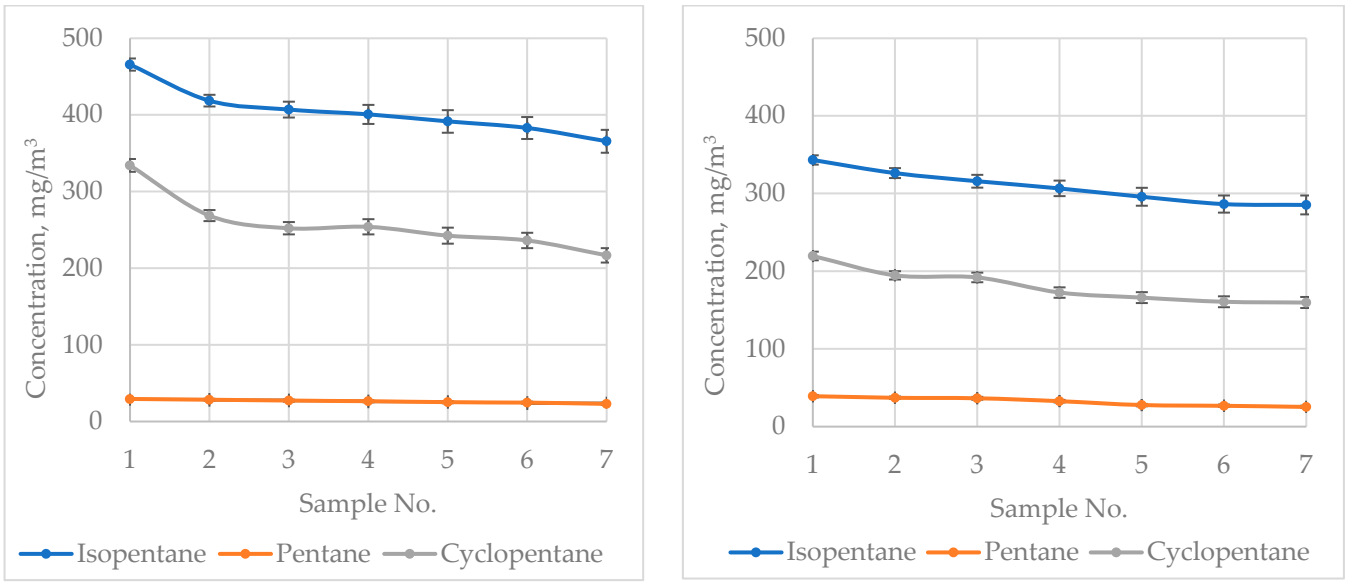

Figure 4. Changes in the gas-phase composition calculated per 1 mg of PIR foam after thermal outgassing of aged samples at 80 °C: (**a**) 6.1–7.9 mg samples; (**b**) 17.5–19.9 mg samples. Error bars indicate standard deviation.

When comparing the curves of gas compositions, we can state that thermal outgassing of a smaller sample in a sealed vial allows for quantifying the amount of released components better. The concentration of pentane is low in the headspace gas, so it is better to use a larger sample to study its release.

After the analysis of heptane extraction samples, it was also decided to increase the mass of the disintegrated samples because the concentrations of pentane mixture components were low in the headspace. The volume of heptane used as the extractant was kept the same—5 mL in the same vials used for headspace analysis. PIR foam samples were increased in mass by approximately 2–2.5 times from 6.1–7.9 mg to 17.5–19.9 mg. The results were calculated as the mass of the extracted component per 1 mg of disintegrated PIR foam in heptane (Table 3).

Table 3. The mass of components released from aged PIR foam during heptane extraction.

16.9–20.4 mg Samples				47.8–53.5 mg Samples			
Sample No.	Isopentane, µg/mg PIR	Pentane, µg/mg PIR	Cyclopentane, µg/mg PIR	Sample No.	Isopentane, µg/mg PIR	Pentane, µg/mg PIR	Cyclopentane, µg/mg PIR
1	0.250	0.108	0.030	1	0.176	0.035	0.017
2	0.218	0.098	0.024	2	0.133	0.023	0.014
3	0.210	0.098	0.022	3	0.197	0.036	0.020
4	0.208	0.094	0.020	4	0.188	0.033	0.019
5	0.200	0.089	0.020	5	0.162	0.036	0.017
6	0.198	0.086	0.020	6	0.115	0.035	0.012
7	0.193	0.083	0.020	7	0.160	0.032	0.016

The results show that a smaller amount of disintegrated sample results in a relatively higher release of gaseous components. This applies for the comparison of released gases calculated per 1 mg of solid material. During milling, it was observed that larger samples of PIR foam disintegrate less effectively, as the foam occupies a large volume due to its low density, and 5 mL of heptane is barely sufficient for effective absorption of released gases. Therefore, the amount of the components that are not dissolved in heptane increases. Due to the higher solubility of isopentane in heptane, the amounts that are not absorbed by heptane are relatively small—an increased amount of PIR material by 2.5 times yields a similar amount of absorbed gases, smaller only by 25%. Meanwhile, the amounts of pentane and cyclopentane in the vapor phase decrease more—when the mass of the disintegrated solid material is increased by a factor of 2.5, the amounts of volatile components absorbed by heptane decrease by a similar factor of 2.5 (calculated per 1 mg of PIR foam).

A comparison of the headspace vapor composition after disintegration of PIR foam samples in heptane is presented in Figure 5. The figure shows that when larger amounts of disintegrated solid material are used, the variation in gas composition is quite scattered, the data lack good reproducibility, and the concentrations of pentane and cyclopentane are significantly lower. However, relative standard deviations were quite similar and ranged between 11 and 13% for all three components. Therefore, it is recommended to use smaller mass samples of PIR material for heptane extraction.

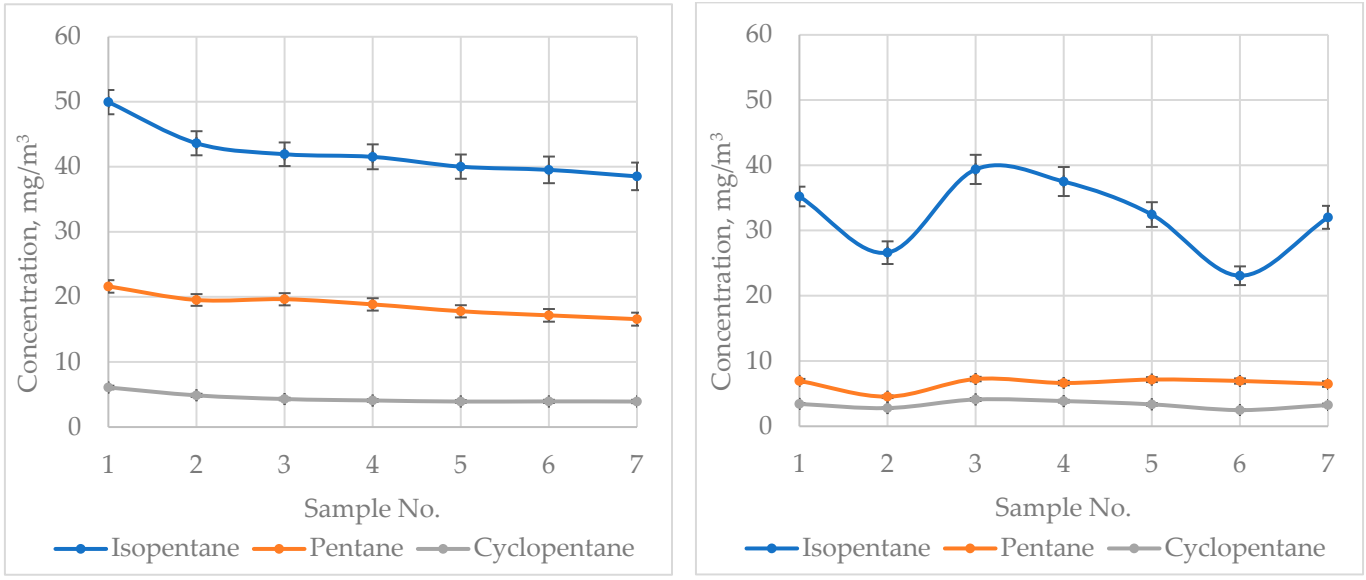

Figure 5. Changes in the gas-phase composition calculated per 1 mg of PIR foam after heptane extraction of aged samples with heptane: (**a**) 16.9–20.4 mg samples; (**b**) 47.8–53.5 mg samples. Error bars indicate standard deviation.

The results show that the thermal outgassing method is the most suitable for qualitative and quantitative analysis of the composition of blowing gases, even though not all the gases present in the foam pores are released during this process. To increase the sensitivity of the analysis, it was decided to investigate the effect of the thermal outgassing temperature on the gas composition. The highest possible temperature that does not cause thermal degradation of the PIR foam was chosen—100 °C. Samples weighing 5.8–7.9 mg were used for the analysis, and the masses of the components released per 1 mg of heated PIR foam are presented in Table 4.

Table 4. The mass of components released from aged PIR foam during thermal outgassing.

80 °C Thermal Outgassing				100 °C Thermal Outgassing			
Sample No.	**Isopentane, µg/mg PIR**	**Pentane, µg/mg PIR**	**Cyclopentane, µg/mg PIR**	**Sample No.**	**Isopentane, µg/mg PIR**	**Pentane, µg/mg PIR**	**Cyclopentane, µg/mg PIR**
1	4.517	0.285	3.242	1	7.998	0.625	5.065
2	4.061	0.276	2.606	2	7.516	0.600	4.909
3	3.948	0.265	2.446	3	6.331	0.472	4.168
4	3.887	0.256	2.464	4	6.042	0.459	3.949
5	3.798	0.245	2.352	5	5.324	0.408	3.510
6	3.715	0.238	2.291	6	5.221	0.391	3.161
7	3.547	0.223	2.103	7	5.042	0.406	3.150

However, when the temperature increases, the amounts of components released into the gaseous phase increase significantly, while the ratio between the components remains the same. This means that the components are released uniformly, and increasing the temperature does not affect the quality of the analysis; however, the increased temperature enhances the sensitivity of the analysis, allowing for the detection of greater changes in the composition of the headspace gas and the investigation of their impact on the quality parameters of thermal insulation materials. Also, it is worth mentioning that higher outgassing temperature yielded better reproducibility of GC/MS results as relative standard deviations were lower for all three components—up to 5.1% for isopentane, up to 5.2% for cyclopentane, and up to 11.1% for pentane.

Changes in the composition of the headspace gas at different thermal outgassing temperatures are shown in Figure 6.

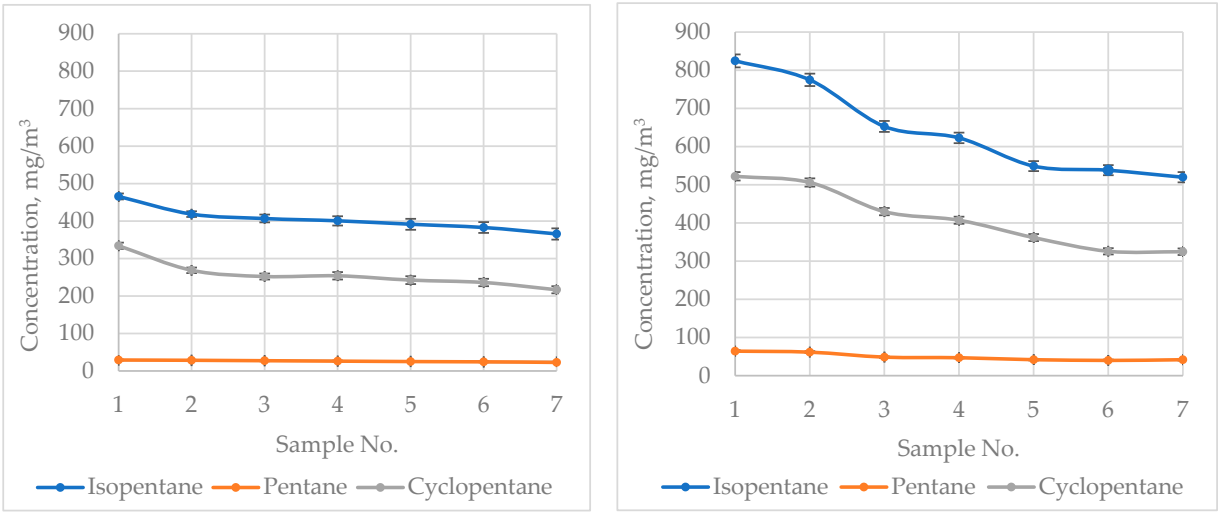

Figure 6. Changes in the gas-phase composition calculated per 1 mg of PIR foam after thermal outgassing of aged samples at 80 and 100 °C: (**a**) 80 °C thermal outgassing; (**b**) 100 °C thermal outgassing. Error bars indicate standard deviation.

3.4. Relation Between PIR Thermal Properties and Gas Diffusion Mechanism

The results clearly show that the increase in the thermal conductivity coefficient of PIR insulation boards during accelerated aging at +70 °C is directly related to changes in the composition of the gases used for foaming within the porous structure of the material. Thermal conductivity measurements revealed two distinct aging stages: an intense initial stage (up to 40–50 days) and a slower stage approaching stabilization during longer storage periods. Such dynamics are characteristic of closed-cell polymeric foams, whose thermal properties strongly depend on the type and concentration of gases present in the pores.

The rapid increase in thermal conductivity observed during the initial thermal aging stage (up to ~8–15%) may be attributed to the active diffusion of blowing agents from the PIR pores and their gradual replacement by air. Isopentane and cyclopentane have significantly lower thermal conductivity than air, so a decrease in their concentration within the pores inevitably leads to an increase in effective heat transfer. GC/MS analysis results confirm this assumption—it was found that as thermal aging time increases, the concentration of the main blowing components decreases, particularly isopentane, which constitutes the largest portion of the gas phase. It was observed that the decrease in isopentane concentration is more pronounced than that of cyclopentane in both the thermal outgassing and heptane extraction methods. This can be explained by the peculiarities of isopentane's molecular structure: due to its branched structure, it exhibits weaker intermolecular interactions, greater volatility, and faster diffusion through the polymer matrix. Meanwhile, cyclopentane, which has a cyclic structure and stronger intermolecular interactions, is released more slowly, so the change in its concentration during accelerated thermal aging is smaller. These differences explain why the overall composition of blowing gas changes unevenly and why the increase in the thermal conductivity coefficient is not linear throughout the entire thermal aging period.

During further accelerated aging period (60–80 days), the rate of increase in thermal conductivity decreases significantly, and the λ values stabilize in the range of 0.0243–0.0247 W/(m·K). This stabilization indicates that the main diffusion processes reach a state of equilibrium, where the removal of residual blowing gases occurs very slowly or their concentration in the pores becomes too low to significantly affect the thermal properties. This behavior is consistent with GC/MS data showing a gradual but slowing decrease in the concentration of isopentane and cyclopentane.

The study also highlighted the importance of the sampling location for the analysis of gas-phase composition. It was found that samples taken from the center of the boards yielded significantly more reproducible and representative results than samples from the edges of the panels. In the edge zones, the PIR structure is more affected by environmental factors, exhibiting greater brittleness and structural heterogeneity, which complicates the preparation of representative samples and increases the variability of results. Therefore, to ensure a reliable analysis of the composition of the blowing gas, it is recommended to take samples from the inner part of the panels.

A comparison of the two sample preparation methods used—thermal outgassing and heptane extraction—revealed that thermal outgassing method is more sensitive and more suitable for both qualitative and quantitative analysis of gas release. Although the headspace concentrations determined during extraction are lower due to the different solubility of components in heptane, both methods reveal the same general trend—a decrease in the amount of blowing gases with accelerated aging. This confirms that the observed changes are related to actual gas loss processes, rather than solely to the characteristics of the chosen analytical method.

Among the identified blowing gases, isopentane exhibited the most pronounced decrease in concentration during accelerated thermal aging, suggesting that its diffusion from

the foam cells plays a major role in the observed increase in thermal conductivity (Figure 7). The results demonstrate a clear inverse relationship between the total concentration of blowing gases (isopentane) and the thermal conductivity coefficient. As the concentration of low-conductivity blowing gases decreases due to accelerated thermal aging, the thermal conductivity of the PIR foam increases. These results strongly suggest that blowing-agent depletion is a major contributor to the observed increase in thermal conductivity.

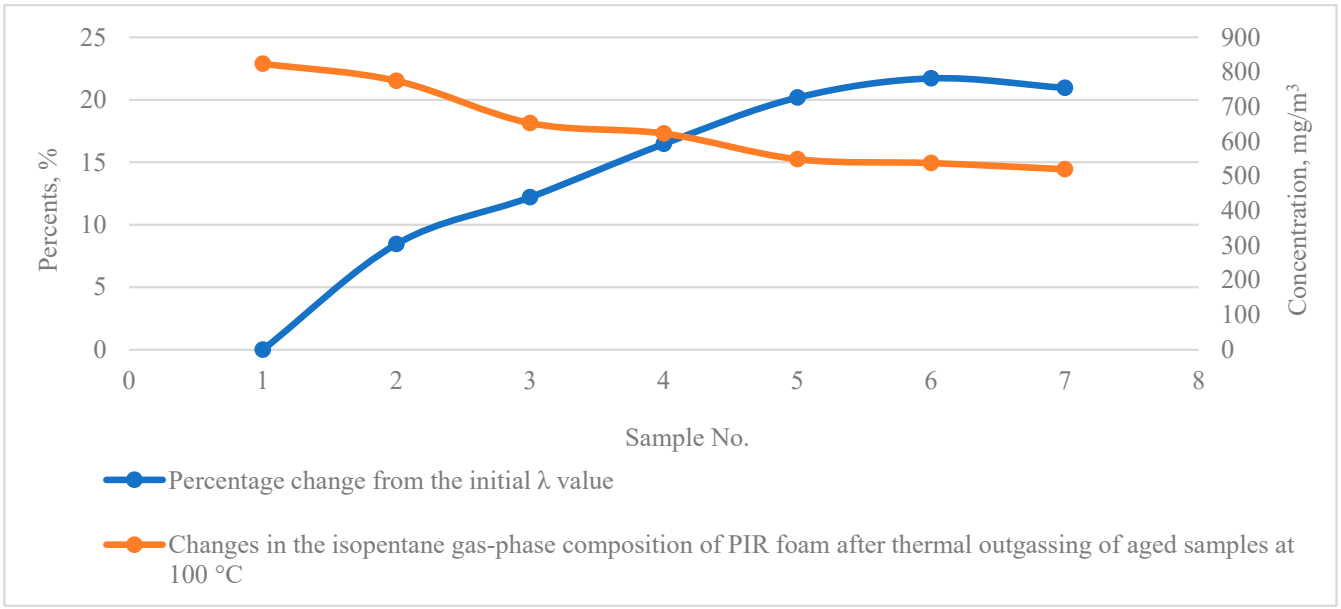

Figure 7. Dependence of measured thermal conductivity change on the experimentally determined concentration of blowing gases in PIR foam.

Although the present results demonstrate a clear relationship between blowing-agent depletion and increasing thermal conductivity, the study did not directly quantify air ingress, moisture uptake, or possible chemical degradation of the polymer matrix. Therefore, the contribution of these mechanisms to the observed accelerated aging behavior cannot be completely excluded and warrants further investigation.

Nevertheless, dependency of thermal conductivity on the gas phase composition can be analyzed through linear regression analysis. Since thermal outgassing yielded the best and the most conclusive as well as the most reproducible results—thermal conductivity was regressed against gas composition after outgassing aged samples at temperatures of 80 °C and 100 °C. The increase in outgassing was calculated as the total increase in all components in the gas phase expressed in percents.

As the results in Figure 8 indicate, there is a strong relation between thermal conductivity decrease and gas phase composition changes after thermal outgassing. Correlation coefficients for both thermal outgassing temperatures are similarly high, exceeding 0.979, which proves that blowing-agent removal from the cells is the most contributing variable to the increase in thermal conductivity of PIR foams.

Further studies have shown that the mass of the sample has a significant effect on the amount of gas captured. Samples with lower PIR mass release relatively more gaseous components, which is attributed to a higher effective surface area-to-volume ratio and more efficient heat and mass transfer. However, this effect is more pronounced for the main foaming components, while in the case of pentane, the dependence on sample mass is less pronounced.

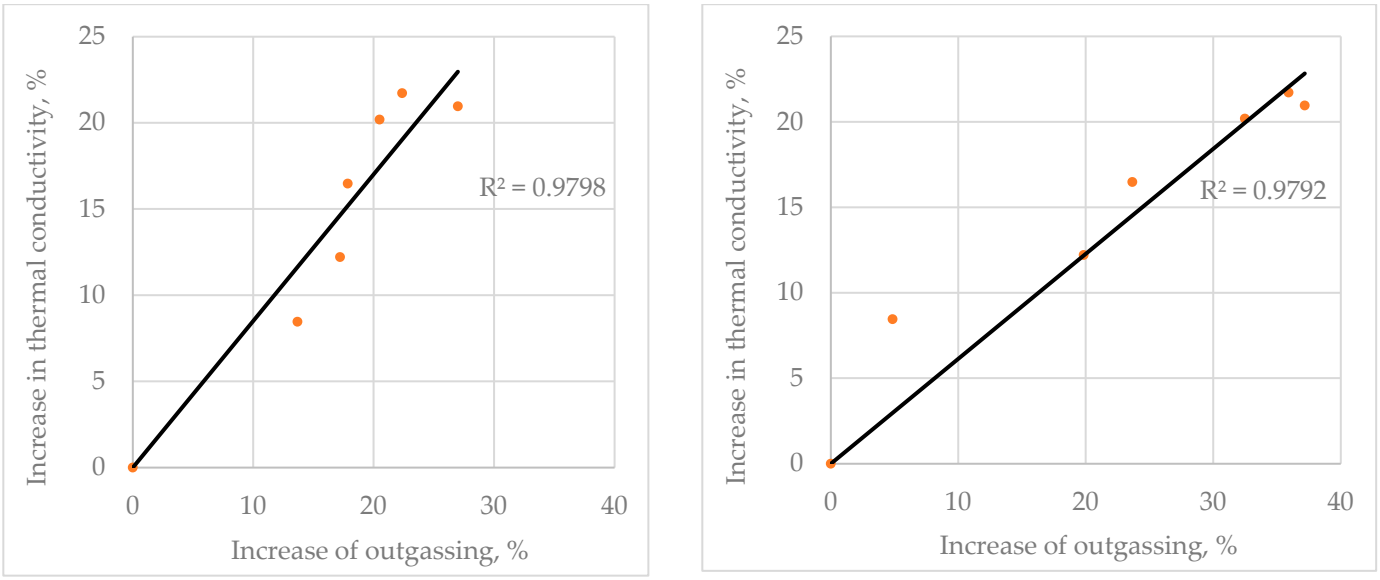

(**a**) (**b**)

Figure 8. Linear regression analysis of PIR foam thermal conductivity dependency on the thermal outgassing of aged samples at 80 and 100 °C: (**a**) 80 °C thermal outgassing; (**b**) 100 °C thermal outgassing.

Increasing the temperature from 80 to 100 °C during thermal outgassing significantly increased the amounts of components released into the gas phase but did not alter their relative proportions. This indicates that a higher temperature accelerates gas desorption and diffusion but does not affect the selective release of components. For this reason, a higher annealing temperature can be considered as a suitable way of increasing the sensitivity of the analysis without compromising data comparability or altering of the gas-phase composition.

In summary, it can be stated that the increase in the thermal conductivity coefficient in PIR boards during accelerated aging is a direct consequence of changes in the composition of the blowing gas. The results of GC/MS analysis provide a molecular basis for explaining these thermal changes and allow for a better understanding of the mechanisms of long-term behavior of PIR insulation materials at elevated temperatures. Such an integrated analysis of thermal and chemical composition is particularly important for assessing the durability of PIR thermal insulation and the evolution of its performance characteristics under real-world conditions.

The present results consistently demonstrate that depletion of blowing agents is the primary mechanism responsible for the increase in thermal conductivity during accelerated aging of PIR foams. The combined thermal conductivity measurements and GC/MS analysis provide complementary evidence supporting this interpretation.

Although all specimens originated from the same production batch and exhibited very similar initial thermal conductivity values prior to thermal aging, future studies including replicate specimens for each accelerated aging period would enable statistical evaluation of experimental variability and further strengthen the robustness of the results.

3.5. Qualitative Optical Microscopy Assesment of PIR Cell Morphology

To complement the thermal conductivity and GC/MS analyses, the cellular morphology of the PIR foam was examined using an optical microscope at 110× magnification. Representative micrographs of the unaged sample (Sample 1) and the thermally aged sample after 80 days at 70 °C (Sample 7) are presented in Figure 9.

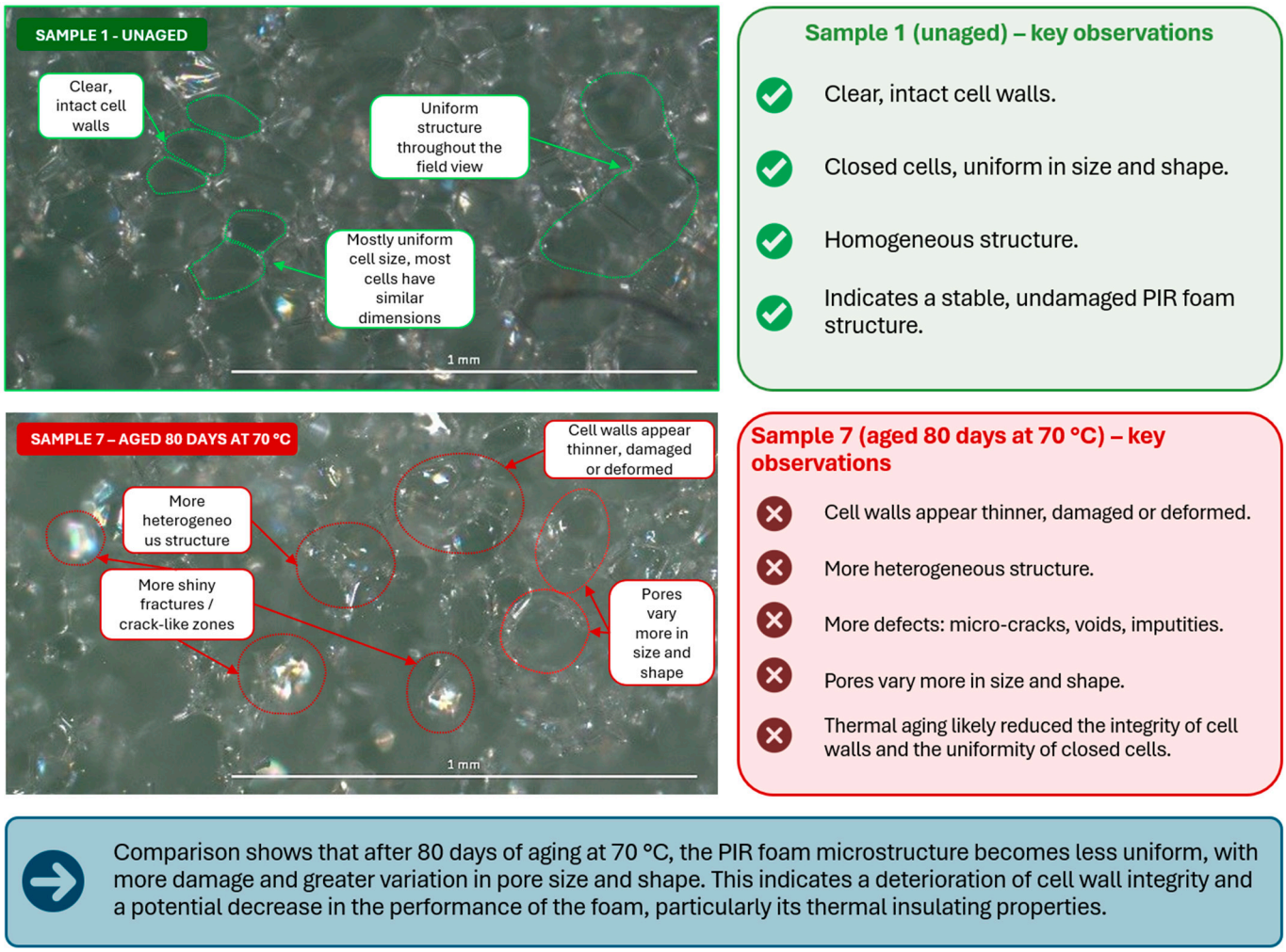

Figure 9. Comparison of the cellular microstructure of unaged and thermally aged PIR foam (110× magnification).

The unaged PIR foam exhibited a relatively homogeneous closed-cell structure with well-defined polygonal cells and continuous cell walls. The cells were generally uniform in size and shape, indicating a stable cellular morphology produced during the foaming process.

In contrast, the aged specimen showed noticeable microstructural changes. The cell boundaries appeared less distinct, and local regions with irregular cell geometry, thinner cell walls and possible micro-defects were observed. The cellular structure also became more heterogeneous, with a larger variation in pore size and shape. Although the majority of cells remained closed, local deterioration of the cellular network suggests partial damage of the polymer matrix after prolonged exposure to elevated temperature.

These observations are consistent with the measured increase in thermal conductivity and the GC/MS results showing progressive depletion of blowing agents. While the dominant aging mechanism is the diffusion of low-conductivity gases from the closed cells, prolonged thermal exposure may also induce minor structural changes that contribute to the deterioration of the insulation performance.

The optical microscopy observations further support the proposed aging mechanism. Although the overall closed-cell morphology was preserved after thermal aging, the aged specimen exhibited a less homogeneous cellular structure with locally deformed cell walls and increased variability in cell geometry. These morphological changes are consistent with previous studies reporting gradual deterioration of the polymer cell network during

prolonged thermal exposure. The observed microstructural evolution is likely to facilitate gas diffusion and may additionally contribute to the increase in thermal conductivity.

4. Conclusions

This study demonstrated that the thermal aging of pentane-blown PIR insulation boards at +70 °C leads to a clear and systematic increase in thermal conductivity, which is directly associated with changes in the composition of the blowing gases trapped within the closed-cell structure. The thermal conductivity coefficient increased from initial values of about 0.0201–0.0211 W/(m·K) to approximately 0.0243–0.0247 W/(m·K) after prolonged thermal aging, corresponding to an overall increase of about 18–22%. The most intensive deterioration occurred during the first 40–50 days of accelerated thermal aging, after which the rate of increase gradually dropped, and the thermal conductivity approached a quasi-stable state.

Gas chromatography–mass spectrometry analysis confirmed that the main gaseous components present in the PIR pores were isopentane, cyclopentane, with smaller amounts of pentane. Accelerated thermal aging caused a progressive reduction in the concentration of these blowing agents, especially isopentane, which showed the most pronounced decrease. This behavior explains the observed increase in thermal conductivity, since the gradual loss of low-conductivity blowing gases and their replacement by air results in less effective thermal insulation.

The results also showed that sample preparation has a significant influence on the reliability of gas analysis. Samples taken from the center of the boards provided more reproducible and representative results than those taken from the edges, where the foam structure was more affected by environmental exposure and mechanical brittleness. Among the two investigated analytical approaches, thermal outgassing proved to be more suitable than heptane extraction for both qualitative and quantitative evaluation of the gas-phase composition, as it provided higher sensitivity and more consistent trends.

In addition, the amount of sample material as well as the thermal outgassing temperature were found to affect the measured gas release. Smaller samples released relatively larger amounts of gaseous components per unit mass, while increasing the outgassing temperature from 80 to 100 °C significantly enhanced the sensitivity of gas detection without changing the relative composition of the released gases. This indicates that higher-temperature thermal outgassing can be used as an effective method for improving analytical sensitivity while preserving comparability of results.

Overall, the results indicate that the loss of blowing agents is a major factor contributing to the deterioration of the thermal performance. The combined thermal conductivity measurements and GC/MS gas analysis provide a consistent explanation of the accelerated aging mechanism and contribute to a better understanding of the long-term behavior of PIR insulation materials exposed to elevated temperatures. These findings are important for assessing the durability and service-life performance of PIR boards in building applications.

In addition to the direct assessment of the accelerated thermal aging mechanisms of PIR thermal insulation materials, the gas composition analysis methods applied in this study open up broader research opportunities. The identified differences in the decline rates of individual blowing gas component concentrations allow for a more detailed analysis of their diffusion processes and their contribution to long-term changes in thermal properties. Such data can be used to develop and refine material aging models and to assess the long-term stability of various blowing gas mixtures.

The results of the study also show that gas-phase composition analysis can be used as an additional tool for assessing the condition and degree of aging of thermal insulation materials. Since changes in gas concentrations are directly related to an increase in thermal

conductivity, it would be appropriate in further studies to explore the possibility of using these relationships to develop indirect methods for evaluating the performance properties of materials. Such an approach would enable the analysis of aging processes based on a smaller number of samples and contribute to the development of long-term studies on the behavior of thermal insulation materials.

Optical microscopy confirmed that prolonged thermal aging resulted in a less homogeneous cellular morphology characterized by locally deformed cell walls and greater variation in pore geometry. These observations complement the GC/MS results and support the conclusion that both blowing-agent diffusion and gradual microstructural degradation contribute to the long-term deterioration of PIR thermal insulation performance.

Author Contributions: Conceptualization, T.M. and A.J.; methodology, T.M. and A.J.; formal analysis, T.M. and A.J.; investigation, T.M., A.J. and J.K.; resources, T.M., A.J., R.B. and J.K.; data curation, T.M., A.J., J.K. and V.Š.-R.; writing—original draft preparation, T.M. and A.J.; writing—review and editing, T.M., A.J., R.B. and V.Š.-R.; visualization, T.M. and A.J.; supervision, R.B. All authors have read and agreed to the published version of the manuscript.

Funding: This research received no external funding.

Data Availability Statement: The original contributions presented in the study are included in this article. Further inquiries can be directed to the corresponding author.

Conflicts of Interest: The authors declare no conflicts of interest.

Abbreviations

The following abbreviations are used in this manuscript:

PIR	Polyisocyanurate
HFOs	Hydrofluoroolefins
CFCs	Chlorolfuorocarbons
GC/MS	Gas chromatography/mass spectrometry

References

1. Değirmenci, B.; Köken, N.; Akar, A. Smoke suppressant and fire-retardant polyurethane-polyisocyanurate (PIR) foam. *J. Appl. Polym. Sci.* **2023**, *140*, e54372. [CrossRef]
2. Chaudhari, D.M.; Stoliarov, S.I.; Beach, M.W.; Suryadevara, K.A. Polyisocyanurate foam pyrolysis and flame spread modeling. *Appl. Sci.* **2021**, *11*, 3463. [CrossRef]
3. Molleti, S.; van Reenen, D. Effect of temperature on long-term thermal conductivity of closed-cell insulation materials. *Buildings* **2022**, *12*, 425. [CrossRef]
4. Yarahmadi, N.; Vega, A.; Jakubowicz, I. Accelerated ageing and degradation characteristics of rigid polyurethane foam. *Polym. Degrad. Stab.* **2017**, *138*, 192–200. [CrossRef]
5. Prałat, K.; Ciemnicka, J.; Jankowski, P.; Wierbicka, E.; Plis, A. Experimental research on the thermal properties of innovative insulation boards made of polyurethane-polyisocyanurate (PUR/PIR). *Pol. J. Chem. Technol.* **2023**, *25*, 40–46. [CrossRef]
6. Berardi, U. The impact of aging and environmental conditions on the effective thermal conductivity of several foam materials. *Energy* **2019**, *182*, 777–794. [CrossRef]
7. Berardi, U.; Madzarevic, J. Microstructural analysis and blowing agent concentration in aged polyurethane and polyisocyanurate foams. *Appl. Therm. Eng.* **2020**, *164*, 114440. [CrossRef]
8. Gama, N.V.; Ferreira, A.; Barros-Timmons, A. Polyurethane foams: Past, present, and future. *Materials* **2018**, *11*, 1841. [CrossRef] [PubMed]
9. Andersons, J.; Modniks, J.; Kirpluks, M. Estimation of the effective diffusivity of blowing agents in closed-cell low-density polyurethane foams based on thermal aging data. *J. Build. Eng.* **2021**, *44*, 103365. [CrossRef]
10. Choi, H.-J.; Ahn, H.; Choi, G.-S.; Kang, J.-S.; Huh, J.-H. Analysis of long-term change in the thermal resistance of extruded insulation materials through accelerated tests. *Appl. Sci.* **2021**, *11*, 9354. [CrossRef]
11. Choi, H.-J.; Kang, J.-S.; Huh, J.-H. A study on variation of thermal characteristics of insulation materials for buildings according to actual long-term annual aging variation. *Int. J. Thermophys.* **2018**, *39*, 2. [CrossRef]

12. Soloveva, O.V.; Solovev, S.A.; Vankov, Y.V.; Shakurova, R.Z. Experimental studies of the effective thermal conductivity of polyurethanen foams with different morphologies. *Processes* **2022**, *10*, 2257. [CrossRef]
13. Malewska, E.; Prociak, A.; Świdzińska-Grela, N.; Kurańska, M. The polyurethane-polystyrene composite-influence of the blowing agent type on the foaming process, the structure and the properties. *J. Compos. Sci.* **2024**, *8*, 135. [CrossRef]
14. Bae, M.; Ahn, H.; Kang, J.; Choi, G.; Choi, H. Determination of the long-term thermal performance of foam insulation materials through heat and slicing acceleration. *Polymers* **2022**, *14*, 4926. [CrossRef] [PubMed]
15. Holcroft, N. Temperature dependency of the long-term thermal conductivity of spray polyurethane foam. *J. Build. Phys.* **2021**, *45*, 571–603. [CrossRef]
16. Jagdev, G.S.; Mukhopadhyaya, P. Temperature-dependent thermal performance of closed-cell foam insulation board in roof constructions. *J. Cold Reg. Eng.* **2020**, *34*, 04020016. [CrossRef]
17. Shrestha, S.; Demchuk, Z.; Polo-Garzon, F.; Tamraparni, A.; Damron, J.; Howard, D.; Saito, T.; Sokolov, A.P.; Hun, D.; Gainaru, C. An experimental toolbox for the physical characterization of thermal insulating polymeric foams. *Heliyon* **2024**, *10*, e36074. [CrossRef] [PubMed]
18. Choe, H.; Choi, Y.; Kim, J.H. Threshold cell diameter for high thermal insulation of water-blown rigid polyurethane foams. *J. Ind. Eng. Chem.* **2019**, *73*, 344–350. [CrossRef]
19. Hermama, C.; Bensiali, B.; Lahbabi, S.; El Maliki, A. Effect of the shape and the distribution of cells on the effective thermal conductivity of polyurethane foam. *Polym. Eng. Sci.* **2023**, *63*, 2278–2294. [CrossRef]
20. Ferkl, P.; Toulec, M.; Laurini, E.; Pricl, S.; Fermeglia, M.; Auffarth, S.; Eling, B.; Settels, V.; Kosek, J. Multi-scale modelling of heat transfer in polyurethane foams. *Chem. Eng. Sci.* **2017**, *172*, 323–334. [CrossRef]
21. Merillas, B.; Villafañe, F.; Rodríguez-Pérez, M.A. Improving the insulating capacity of polyurethane foams through polyurethane aerogel inclusion: From insulation to superinsulation. *Nanomaterials* **2022**, *12*, 2232. [CrossRef] [PubMed]
22. *EN 13165:2012+A2:2016*; Thermal Insulation Products for Buildings-Factory Made Rigid Polyurethane Foam (PU) Products–Specfication. Comité Européen de Normalisation: Brussels, Belgium, 2016.
23. Makaveckas, T.; Bliūdžius, R.; Burlingis, A. Determination of the impact of environmental temperature on the thermal conductivity of polyisocyanurate (PIR) foam products. *J. Build. Eng.* **2021**, *41*, 102447. [CrossRef]